Available online at www.sciencedirect.com

ScienceDirect

journal homepage: www.elsevier.com/locate/issn/15375110

Research Paper

Spectral monitoring of salinity stress in tomato plants

*Timea Ignat, Yoav Shavit, Shimon Rachmilevitch, Arnon Karnieli**

French Associates Institute for Agriculture and Biotechnology of Drylands, Jacob Blaustein Institutes for Desert Research, Ben-Gurion University of the Negev, Israel

ARTICLE INFO

Article history:
Received 18 August 2021
Received in revised form
11 February 2022
Accepted 27 February 2022

Keywords:
non-invasive
machine learning
spectroscopy
Solanum lycopersicum L.
vegetation stress

Water salinity is a widespread agricultural hazard that affects approximately 20% of irrigated land, causing a significant yield reduction in crops. Stress coping mechanisms by plants were thoroughly examined but understanding of plant adaptation and acclimation is still lacking and is often species- and variety-specific. Presently, the biochemical and physiological methods that are used to assess plant stress are costly, destructive, and time-consuming. Alternatively, spectroscopy is a potential method to monitor biochemical components and physiological states of plants. The objective of the current work was to build a spectral-based model for detecting plants under salt stress, in order to optimise plant-status monitoring in a non-destructive manner. In this study, five different tomato graft combinations were examined under four different salinity treatments in a greenhouse. Hyperspectral measurements were conducted in the range of 400–2500 nm, and chemometrics was used for data analysis and modelling. Salt treatments were found to affect the physiological performance of plants, although environmental conditions had a greater influence on plant temporal physiological trends. Spectral data acquisition with chemometrics showed high ability to predict salt accumulation in plants (root mean square error of prediction (RMSEP) of 0.47 mg g^{-1} and 2.8 mg g^{-1} for Na^+ and Cl^-, respectively). Moreover, a hyperspectral, robust decision-supporting classification model was established for detecting plants under salt stress (prediction specificity: 0.94). The presented capabilities of predicting Cl^-, Na^+, and the K:Na ratio in a non-destructive manner, by utilising spectroscopy, could serve as the basis for developing a low-cost, fast, and efficient stress detection method, independent of environmental conditions.

1. Introduction

Plant stress can be described as an external biotic or abiotic suppressor that limits photosynthesis. The major abiotic stresses, such as high salinity, drought, cold, and heat, negatively influence the survival, biomass production, and yield of staple food crops by up to 70% (Vorasoot et al., 2003; Kaur et al., 2008; Ahmad et al., 2010; Thakur et al., 2010; Mantri et al., 2012). Soil and irrigation water salinity are a widespread

* *Corresponding author*. Jacob Blaustein Institutes for Desert Research, Ben-Gurion University of the Negev, Sede Boker Campus, 84990, Israel.
E-mail address: karnieli@bgu.ac.il (A. Karnieli).

https://doi.org/10.1016/j.biosystemseng.2022.02.018
1537-5110/

agricultural hazard that affects approximately 20% of irrigated land, causing a significant crop yield reduction (Qadir et al., 2014). Water and soil salinisation tend to be common in arid and semi-arid regions, where salt leaching is inadequate due to low rainfall (Pitman & Läuchli, 2006).

Plant adaptation to environments with excessive salt concentrations occurs due to the activation of physiological and biochemical coping mechanisms, leading to the most efficient ion and water homeostasis regulations (Hasegawa et al., 2000). These mechanisms include regulations over plant growth rates (Maggio et al., 2002), ion compartmentation (Niu et al., 1995; Zhu, 2002), and osmotic adjustments (Morgan, 1984; Yancey, 2004). Even though these mechanisms have been thoroughly examined and characterised, the understanding of plant adaptation over multiple generations and dynamic acclimation processes, involving physiological, anatomical and morphological adjustments, is still lacking, and the knowledge that does exist is usually species-specific or even variety-specific. In sum, plant adaptations to stress and root-zone salinity affect crop yield (Hasegawa et al., 2000; Hsiao, 1973). Therefore, there is a worldwide demand for agro-techniques and breeding solutions to enhance crop productivity under environmental stress. One approach in meeting the current environmental challenges is to develop abiotic-stress-tolerant crops using breeding methods. A different approach is the use of grafting technique, which has been gaining popularity worldwide (Aidoo et al., 2018; Kubota et al., 2008; Lee et al., 2010; Lee & Oda, 2003). Additionally, due to the limited availability of arable land and the high market demand for vegetables around the world, crop production is expanding into areas with less favourable soil and environmental conditions that constitute the most limiting conditions for agricultural productivity worldwide (Schwarz et al., 2010).

The consistent reductions in the physiological variables' performances, such as leaf water content, stomatal conductance, and photosynthesis, are the results of the two-phase growth (phase 1: osmotic stress, phase 2: salt-specific effect) response to excessive salinity described by Munns (2005). Once salt stress is applied, there is a reduction in plants' ability to take up water, which leads to stomatal closure and photosynthetic inhibition, a phase also known as the osmotic effect. Salts taken up by the roots into the plant concentrate in old leaves and continue moving into transpiring leaves. Shoot salt partitioning in old leaves was suggested to be a salt-tolerance mechanism that protects the younger, most active leaves (Di Gioia et al., 2013).

Elevated Na^+ levels in the root medium reduce nutrient assimilation, mainly of K^+, Ca^{2+} (Zhu, 2001), and Mg^{2+}. The K^+ uptake disturbance by Na^+ damages stomatal regulation and ultimately causes water loss through the stomata. On the other hand, Cl^- is seen by some as a more toxic ion when reaching high levels, causing a reduction in chlorophyll production that results in a non-stomatal photosynthetic capacity loss (Tavakkoli et al., 2011). In tomato, salinity reduces leaf K^+, Ca^{2+}, and Mg^{2+} concentrations. Plants that take up more K^+, Ca^{2+}, and Mg^{2+} from the medium are considered to be better adapted or acclimated (Cuartero et al., 1992; Pérez-Alfocea et al., 1996).

Tomato (*Solanum lycopersicum* L.) is one of the world's major fresh and processed fruits and is the second most important agricultural vegetable after potato (FAOSTAT, 2018). Tomato production, with the highest global yields, is concentrated in a few warm, arid, and semi-arid regions. Over 30% of worldwide production is located in countries surrounding the Mediterranean Sea and approximately 20% in California (FAOSTAT, 2018). Tomato is a moderately salt-tolerant plant that can attain a yield within an electrical conductivity (EC) range of 1.3–6 dS m^{-1} and is typically cultivated in salinisation-exposed environments (Cuartero & Fernández-Muñoz, 1998). The response of tomato to salinity has been documented and still constitutes an ongoing research topic (Estañ et al., 2005). Excess soil and water salinity in tomato production causes several effects, such as root biomass decrease (Papadopoulos & Rendig, 1983), delay in seed germination, inhibited plant growth, and yield reduction (Dalton et al., 2001; Romero-Aranda et al., 2002). Inhibition of tomato leaf growth in salinised soils was found to correlate with a reduction in cellular turgor and photosynthetic activity (Munns, 2002). Tomatoes, like other spring-summer crops of Mediterranean zones, are usually affected not only by the high salt concentration in the root-zone but also by additional environmental factors, such as high temperatures and low relative humidity, that may have an additive effect on the growth and yield inhibition (Johnson et al., 1992). Previous studies demonstrated a reduction of 10% in fruit weight resulting from irrigation water with EC of 5–6 dS m^{-1}, and a reduction of 30% under an 8 dS m^{-1} EC salt treatment. Low yield was also attributed to salinity's effect on the plants' reproductive organs, causing flowering inhibition, a reduced number of fruits per plant, and a decrease in pollen viability (Grunberg et al., 1995).

The most prevalent current methods used to assess instantaneous plant stress states are physiological or laboratory measurements, although often, they may be costly, destructive, and time-consuming. An alternative rapidly developing method for plant stress detection is spectroscopy, which is based on light energy absorption. Within the visible wavelength range (VIS, 400–700 nm), the major absorbers are pigments, while water, carbohydrates, fats, and proteins have absorption bands in the near and shortwave infrared (NIR, 750–1000 nm; SWIR, 1000–2500 nm, respectively) regions. In general, the VIS-, NIR-, and SWIR spectral signatures vary for species, and they depend on leaf maturity, physiological state (due to differences in pigment levels), moistness, air content, and anatomical arrangements of leaf cells (in particular mesophyll cells), among other factors (Gausman, 1984). Hyperspectral measurements in the range of 350–2500 nm have proven, in the last decade, to potentially be an effective tool in the field of precision agriculture, either by proximal or remote estimation of biochemical variables in plants (Cochavi et al., 2017; Hernández et al., 2014; Rapaport et al., 2015; Herrmann et al., 2020). In order to establish an effective spectral detection tool, preliminary knowledge is needed, based on high spectral resolution spectrometers and machine learning algorithms. This learning and calibration process can be time consuming and costly, but may provide information that is collected non-destructively and is linked to plant biochemistry and physiology based on specific bands (Das et al., 2020; El-Hendawy et al., 2019). This knowledge can be used to develop low-cost, remote, soft sensor applications for prediction of vegetation's internal components and stress

level (Brunner et al., 2021). Several studies have been conducted linking spectral signature with biochemical and physiological changes. Concerning stress, Rapaport et al. (2015) showed that in grapevines, combining the spectral responses in the VIS (531 nm) and SWIR (1500 nm) regions yielded a superior ability to predict physiological values at both the leaf and the canopy levels. These models using the novel water balance index also demonstrated applicability for water status monitoring and irrigation scheduling under field conditions. Moreover, Rapaport et al. (2015) found a significant correlation between plant spectral and physiological properties, such as leaf water potential, stomatal conductance, and non-photochemical quenching, indicating the predictive potential of physiological characteristics in a non-destructive manner. In a salt stress experiment conducted in eggplant, Leone et al. (2007) demonstrated, by spectral measurement in the range of VIS-NIR, the predictive potential for soil properties (pH and EC). Significant relationships were obtained between plant characteristics, such as biomass, leaf area index, and water and chlorophyll contents, and vegetation indices. Increasing ion concentrations in saline-stressed wheat and sugarcane were monitored in the works of Steidle Neto et al. (2017) and El-Hendawy et al. (2019) using hyperspectral measurements. In melon plants throughout the spectral range of VIS-NIR, Hernández et al. (2014) demonstrated that the normalised difference vegetation index ($NDVI_{750-705}$, based on 705 and 750 nm) and the ratio between the water index (WI, based on 900 and 970 nm) and the normalised difference vegetation index ($WI{:}NDVI_{750-705}$) showed significant relationships ($p < 0.01$) with salinity. Hyperspectral measurements have demonstrated potential to monitor and predict the physiological state of plants under stress (Rapaport et al., 2015; Rodríguez-Pérez et al., 2007; Serrano et al., 2010) in a non-destructive manner. Nonetheless, studies about improved stress detection analysis and modelling are still required due to the different spectral signatures yielded by different species and stress agents (Carter & Knapp, 2001). Established prediction models for stress detection can potentially be applied in large-scale precision agriculture by spectroscopic methods.

Most studies mentioned above have been conducted at a single time point or in a relatively short time period. In these timeframes and under controlled environmental conditions, physiological measurements have been found to describe well the stressed plant's status. In case of longer-term cultivation, together with continuous plant stress and under varying environmental conditions, physiological measurements tend to be mainly linked to the plant's temporal state and lack the ability to reflect the plants stress status. The present study addresses the complexity of plants coping with saline stress, along with varying environmental conditions, and demonstrates the hyperspectral measurement technique's ability to reliably determine vegetation salinity stress under such conditions.

The objectives of the present work were to evaluate the salt stress effects on the physiology and biochemical variables of tomato plants and to study the ability of hyperspectral measurements to predict plant stress caused by salinity. Furthermore, it aimed to establish an environment-independent chemometric model for a decision support system to predict saline stress levels in tomato plants.

2. Materials and methods

The study experiments took place at Ben-Gurion University of the Negev's Sede Boqer Campus. The study site (30°51′14.21″N, 34°47′1.3″E) is located in a tomato-growing region in Israel's Negev Desert with an annual rainfall average of 80 mm. The annual mean temperature is 18 °C, and the average relative humidity at 14:00 is between 20 and 30%. Two experiments were conducted inside a nearly commercial-size (50 × 70 m) net-house with a polyethylene cover, with 50-mesh net on the sides to prevent pest penetration, and without an active environmental control system. The first experiment was conducted between March 26 and June 18, 2018 while the second experiment through January 13 to March 3, 2020. The durations of the first and second experiments were 82 and 50 days, respectively.

2.1. Plant materials

In the first experiment, four different tomato (*S. lycopersicum* L.) varieties were used in different grafting combinations. Varieties were chosen based on commercial use and salinity tolerance. The Ikram cluster-tomato (Syngenta Seeds, Milan, Italy) cultivar was solely used as a scion in the experiment due to its wide commercial usage. Additionally, Ikram is known as a vigorous cultivar with a high yield, long shelf life, and resistance to Fusarium Wilt, Verticillium Wilt, and Tobacco Mosaic Virus. The rootstock varieties were as follows: (1) Beaufort (De Ruiter Seeds, Netherlands), the most common tomato rootstock worldwide with vigorous growth capabilities; (2) Resistar (Hazera Seeds Ltd., Israel), a commercial rootstock that has been shown to have increased yield at low salinity levels (Savvas et al., 2011); (3) TRS-2 (TomaTech Ltd., Israel), a non-commercial, experimental variety; and (4) Ikram. In the second experiment, for the chemometric model validation, the Shiran cultivar was used as rootstock. Plant materials were supplied by Hishtil Nurseries (Ashkelon, Israel).

2.2. Experimental setup

Seedlings were planted in 24 L volume bucket-shaped pots embedded with rock wool. Plant containers were filled with sand, the predominant soil type in the region for tomato cultivation. Irrigation was controlled by an irrigation computer, enabling 15-min cycles, through a 2 L h^{-1} dripper (Netafim, Israel). Each plant had three drippers and four irrigation cycles were taking place per day throughout the experiments. A RollerHook Tomato Vine Crop Trellis was used to support the plants. Due to the sand's physical nature, percolation and drainage were rapid, necessitating excess irrigation, reaching 6 L of water per day per plant. Fertilisation was performed with each irrigation cycle, providing macronutrients (N–P–K (17%-10%-27%), $N{-}NO_3$ (11.3%) and P_2O_2 (10%)) and micronutrients (29%) (Poly Feed; Haifa Chemicals, Israel). A fertiliser pump (Tefen, Israel) supplied irrigation water with a fixed 0.2% of fertiliser, reaching a final macro- and micronutrients concentration ratio of 500 mg L^{-1}. Saline solution was prepared in an 80 L tank with 125,000 mg L^{-1} NaCl

concentration. The NaCl solution was pumped from the tank to irrigation pipes by three adjustable hydraulic pumps (0.4%–4%), one for each saline treatment. The electrical conductivity of the irrigation water emerging from the drippers was measured once a week for all treatments using a field EC meter (WTW GmbH and Co., Germany) that was calibrated with the Lab Con 510 EC m (Eutech Instruments, Nijkerk, Netherlands). Drinking water was used for irrigation. The pH of the irrigation water applied after adding macro- and micronutrients, was 6.7.

In both experiments, the non-destructive physiological and hyperspectral measurements were first completed on the youngest fully mature leaf and a basal leaf while the leaves were still attached to the plants. They were followed by the destructive laboratory measurement sampling by harvesting the same leaves. Seedlings were planted at the age of 14 days and were cultivated with control (EC 1.2 dS m^{-1}) irrigation for up to 22 days when the treatments began.

The first experiment contained four replicates of the four different salinity treatments with mean values of EC equal to 1.2 (control, without added NaCl), 3, 6, and 9 dS m^{-1}. An open-loop cultivation system was used in which leachate was discharged to the ground. Environmental conditions were recorded using a relative humidity and temperature sensor (DHT22 - AM2302, Guangzhou Aosong Electronic Co., Ltd., China) located at the height of the trellising cable between the rows in order to accurately represent the conditions sensed by the plants. The temperature and relative humidity data were recorded every minute. Measurements started six days after treatment (DAT) and ended 62 DAT. Altogether, 80 plants were monitored in bi-weekly, alternating manner. Plants 1–40 were measured and sampled on the odd weeks, while plants 41–80 on the even weeks. On each plant the youngest fully mature leaf and one basal leaf were sampled.

During the second experiment, the growth conditions were similar to the first experiment, and the applied salinity treatments were EC 3 dS m^{-1} and EC 9 dS m^{-1}. The measurements were only taken at the end of the experiment on 28 DAT. The youngest fully mature leaf and the basal leaf of 12 plants were scanned in the same manner as in the first experiment. Since Cl^- is feasible to quantify and it represents well the salinity stress in plants; therefore, the second experiment was only used for validating the chemometric model for Cl^- accumulation in the plants.

2.3. Leaf physiological performance

A LICOR 6400 portable photosynthesis system (LICOR, Lincoln, NE, USA) was used for measuring stomatal conductance (g_s; mol H_2O m^{-2} s^{-1}), leaf transpiration rate (E; H_2O m^{-2} s^{-1}), efficiency of photosystem II (PhiPS2), leaf vapor pressure deficit in the leaf vicinity (VPD_{leaf}), and photosynthetic carbon net assimilation (P_N; μmol CO_2 m^{-2} s^{-1}). The variable settings were as follows: a concentration of 400 μmol mol^{-1} was set in the reference cell; the molar flow rate of air entering the leaf chamber was set to 500 μmol s^{-1}; cell temperature was fixed at 25 °C; photosynthetically active radiation (PAR; μmol s^{-1} m^{-2}) was fixed at environment photosynthetically active radiation during measurements, approximately 900 μmol s^{-1} m^{-2}, with 10% of blue light; and the stomatal ratio was set to 0.2. From 6 to 62 DAT, physiological data acquisition occurred on a weekly basis.

2.4. Chemical analysis

In order to examine the rootstocks' abilities to include or exclude toxic ions, leaf chloride concentration measurements and inductively coupled plasma (ICP) assays were conducted.

Aiming at preparing samples for Cl^- concentration measurements and ICP, the dried leaflets were separated from their petioles and primary rachis, and were ground and homogenised using stainless steel milling balls in a Mixer Mill MM 400 (Retsch, Haan, Germany) set for 1 min at 22 Hz. The ground samples were weighed on a Sartorius CP225D analytical scale (Sartorius, Goettingen, Germany) with five-digit accuracy and distributed to each assay according to the protocols.

For chloride concentration assessment, samples were weighed (~0.1 g) into 15-mL corning tubes, and 10 mL of double-distilled water (DDW) was added to each tube. Samples were placed on an MRC TOS-4030FD shaker (MRC Lab, Germany) for 12 h, operating with 140 spins per minute. Samples were filtered through a Whatman-40 filter paper (Whatman International Ltd., Maidstone, England). Chloride concentration was determined from 0.5 mL of filtrate by a chloride analyser (Chloride Analyser mod. 926, Sherwood Scientific Ltd., Cambridge, UK). Chloride concentration was expressed in mg g^{-1}.

The elemental analysis was done by ICP analytical technique. Sample preparation followed the accelerated wet digestion protocol of Campbell and Plank (1998), and the samples were analysed at an external laboratory using a Varian 720-ES inductively coupled plasma optic emission spectrometer (Varian Inc., Palo Alto, CA, USA). Since the preparation process was time-consuming and costly, the ICP assay was performed on 73 samples, on the youngest fully mature leaves and the basal leaves at 27 DAT.

2.5. Hyperspectral leaf reflectance

Leaf reflectance was obtained by an Analytical Spectral Device (ASD) spectroradiometer FieldSpec Pro FR (Analytical Spectral Devices, Inc., Boulder, CO, USA). The system was set to measure the reflectance mode in the 350–2500 nm range, at a 1-nm spectral sampling rate with a spectral resolution of 3 nm at 350–1000 nm and 10 nm at 1001–2500 nm. As a reference, a Spectralon diffuse reflectance standard target (99%) (Labsphere, North Sutton, NH 03260 US) was used, and measurements were obtained on a regular basis after every fifth scan. The reflectance target was measured after being attuned to the environmental conditions. Leaf spectral measurements (average of five scans) were acquired by a plant probe with an internal light source together with a leaf clip (Analytical Spectral Devices, Inc., Boulder, CO, USA). The light direction was perpendicular on the leaf, and the reflectance signal was collected in 45° by the fibre optic. The warm-up time was

40 min prior to the measurements for the spectrophotometer and light source alike.

Spectral measurements were performed on a young fully mature leaf and a basal leaf once a week at mid-day. In order to eliminate local spectral variance, each leaf was sampled on three different compound leaflets, avoiding the terminal leaflet. To enhance the spectral signature differences, pre-processing was applied based on Savitzky–Golay's (Savitzky & Golay, 1964) method: second derivative, window size: 7 and polynomial order: 2 (D_2R).

2.6. Chemometrics

A statistical analysis to examine differentiating between treatments was performed using R Statistical Software (version 3.4.3; R Foundation for Statistical Computing, Vienna, Austria). The Levene's test for homogeneity of variance and the Shapiro–Wilk test for normal distribution of residuals were performed. Comparisons of means for all treatments were performed using the Tukey-HSD multi-comparison test. Statistical significance between treatments was distinguished by lower-case letters based on confidence intervals ($p = 0.05$).

The partial least squares-regression (PLS-R) and the partial least squares-discriminant analysis (PLS-DA) models were performed using the PLS toolbox (PLS, Eigenvector Research, Wenatchee, WA, USA) and were run under MATLAB 2019b software (MathWorks, Natick, MA, USA). Regression models were formulated to link the spectral information to the internal components. The error associated with the regression model's results were defined by the root mean square error of calibration (RMSEC):

$$RMSEC = \sqrt{\frac{\sum_{i=1}^{n}\left(\hat{y}_i - y_i\right)^2}{n}} \quad [1]$$

where $\hat{y}_i$ is the predicted value of the internal component of sample i, y_i is the value of internal component of sample i, and n is the number of calibration samples. RMSEC is a measure of how well the model fits the data.

Root mean square error of cross-validation/prediction (RMSECV/RMSEP) is a measure of a model's ability to predict new samples. The RMSECV/RMSEP is defined as in Eq. (1), except that $\hat{y}_i$ are predictions for samples not included in the calibration model. RMSECV used data from cross-validation, while RMSEP used data from the independent validation dataset. RMSE is expressed in the unit of the related internal components or physiological measure. Cross-validation was performed by using Venetian blinds, random data split (ten data split). During the machine learning process in the first experiment the dataset (n) in each case was randomly divided into two groups: 70% for model building (calibration (Cal) and cross-validation (CV)) and 30% for external validation (Pred). The data from the second experiment was used for model validation.

The statistical measure of the performance of the PLS-DA classification were sensitivity and specificity. Sensitivity is a measure of how often the test correctly identifies a positive among all positives (Eq. (2)), while specificity (Eq. (3)) is a measure of how accurate a test is against false positives. Specificity can be considered as the percentage of the times a test correctly identifies a negative result. For the PLS-DA, the dataset was divided in the same manner as for the PLS-R.

$$Sensitivity = \frac{true\ positives}{(true\ positive + false\ negative)} \quad (2)$$

$$Specificity = \frac{true\ negatives}{(true\ negative + false\ positives)} \quad (3)$$

The machine learning procedure using PLS-R was as follows: the regression model was built on one particular DAT measurement, followed by model adaptation for an extended dataset of different DATs and leaf locations on plants. It means that the learning procedure started on the youngest fully mature leaves for a particular DAT in order to learn how the chemical compound change in the leaves is reflected on the spectral signature. This process included wavelength range selection for each chemical compound in order to achieve the models' highest prediction ability. The wavelength selection was done in an iteration manner during the PLS-R regression process. The next step in the learning procedure was to extend the existing PLS-R model with data from different DAT and further on with leaves that are different in age. The last step of the procedure was to validate the models with samples that were not taking part in the model building process.

3. Results

The detailed results are shown for the first experiment. Results that are related to the second experiment are specifically noted.

3.1. Meteorological measurements

Throughout the experiment, the highest and lowest measured temperatures were 46.7 °C on May 18, 2018 (31 DAT) and 10.6 °C on April 22, 2018 (5 DAT). During the last week of April (7–13 DAT) and the first two weeks of May (14–27 DAT), the temperature maintained an oscillating rhythm with relatively large differences between high and low temperature values. From mid-May (28 DAT), the oscillation rhythm diminished (Fig. 1a), and its effect could be seen very distinctly in the gradually increasing and decreasing values of PhiPS2.

Due to the microclimate conditions formed in the net-house environment, the relative humidity in most nights reached a maximum of 100% and a minimum of 12.1% on May 18, 2018 (31 DAT) during the day. The oscillation rhythm of the relative humidity minimum values during the day was stable throughout the experiment, reaching low values in the beginning of May to mid-May and the beginning of June (Fig. 1b). Low humidity values occurred on April 30, 2018 (13 DAT) and May 23, 2018 (36 DAT).

Similar to temperature, the vapor pressure deficit of the air (VPD_{air}) (Fig. 1c) maintained a high oscillation rhythm up until mid-May (28 DAT) and was more stable from that point until the end of the experiment.

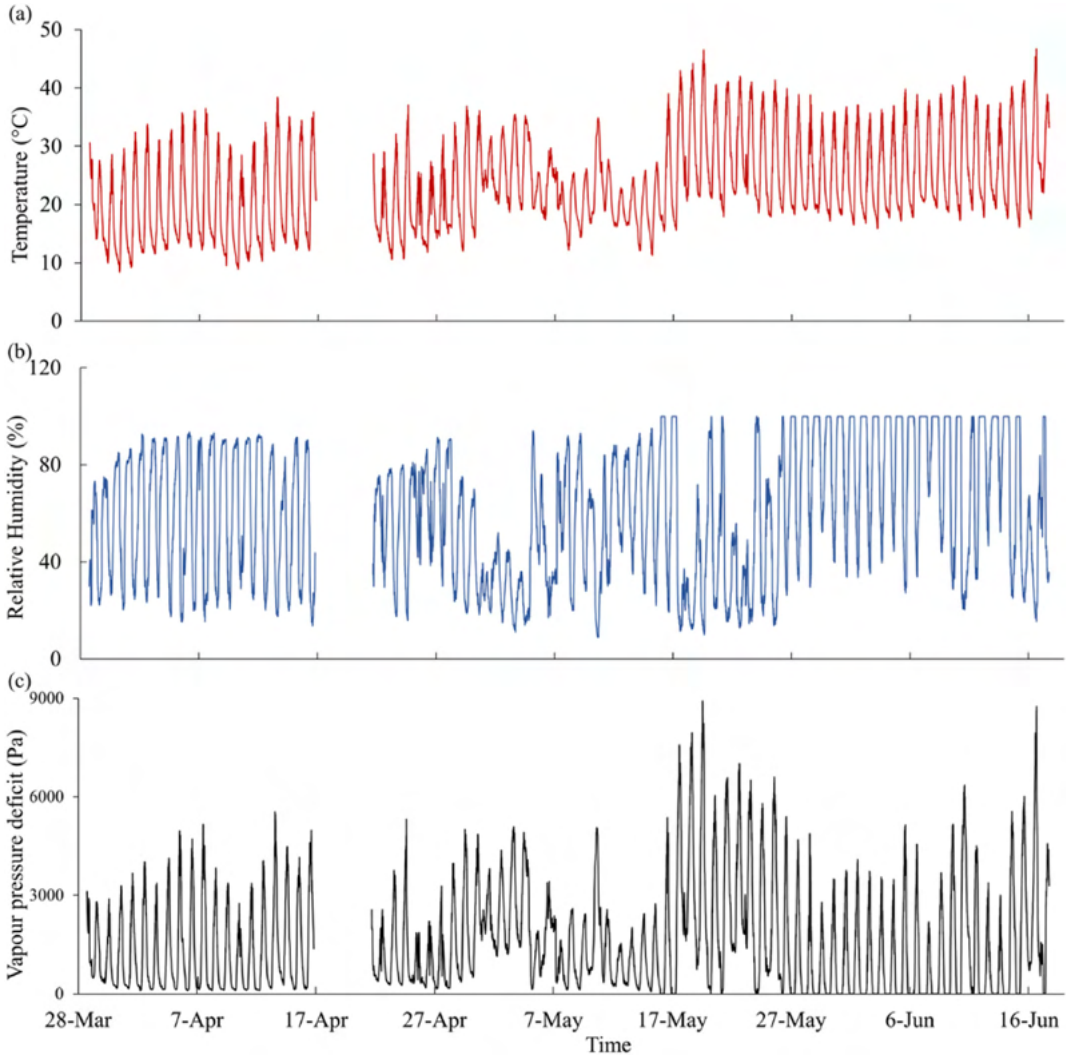

Fig. 1 – Net-house environment temperature (a), relative humidity (b), and vapor-pressure deficit (air) (c) values attained during the measurement campaigns with 10-min resolution.

3.2. *Physiological performance*

Stomatal conductance (g_s) (Fig. 2a) values measured in leaves showed decreases of 13, 47, and 56% between the control and the EC 3, EC 6, and EC 9 treatments, respectively, for the youngest fully mature leaves 37 DAT. Decreasing g_s differences were found between the youngest fully mature leaves and the old leaves towards the end of the experiment, especially under the mild salt treatments (i.e., control and EC 3). The VPD_{air} peaks (Fig. 1c) that appeared at high temperatures and low relative humidity correlated well with g_s (Fig. 3) and resulted in decreasing photosynthetic activity.

Similarly to g_s, the photosynthetic rate (P_N) (Fig. 2b) decreases due to salt stress observed from 6 DAT, and significant differences were first seen 27 DAT. Differences of 17, 34, and 40% were noticed between the P_N of the control and the EC 3, EC 6, and EC 9 treatments, respectively, 37 DAT. On several measurement campaign dates, EC-3-treated plants demonstrated P_N that was equal to or higher than the control treatment. These results suggest that low salt concentrations, such as 3 dS m^{-1}, may not cause noticeable physiological differences. The P_N ratio of the youngest fully mature leaves and the basal leaves increased throughout the experiment.

Through the course of the experiment, the transpiration rate (E) (Fig. 2c) demonstrated similar behaviour to g_s, showing a trend of decrease of 7, 32, and 38% between the control and the EC 3, EC 6, and EC 9 treatments, respectively, for the youngest fully mature leaves 37 DAT. Although very similar in their trends, 37 DAT, E showed a high rate of activity, while stomatal conductance decreased.

Measured VPD_{leaf} reached its highest values on hot days when the temperature reached 41.2 °C. Results showed an increasing trend of VPD_{leaf} as the NaCl concentration increased in the irrigation. VPD_{leaf} was shown to be linked to VPD_{air} measured in the net-house (Fig. 1c), demonstrating significant changes between treatments on days with high temperatures and low relative humidity. Regarding leaf position, bottom leaves demonstrated higher VPD_{leaf} than the youngest fully mature leaves.

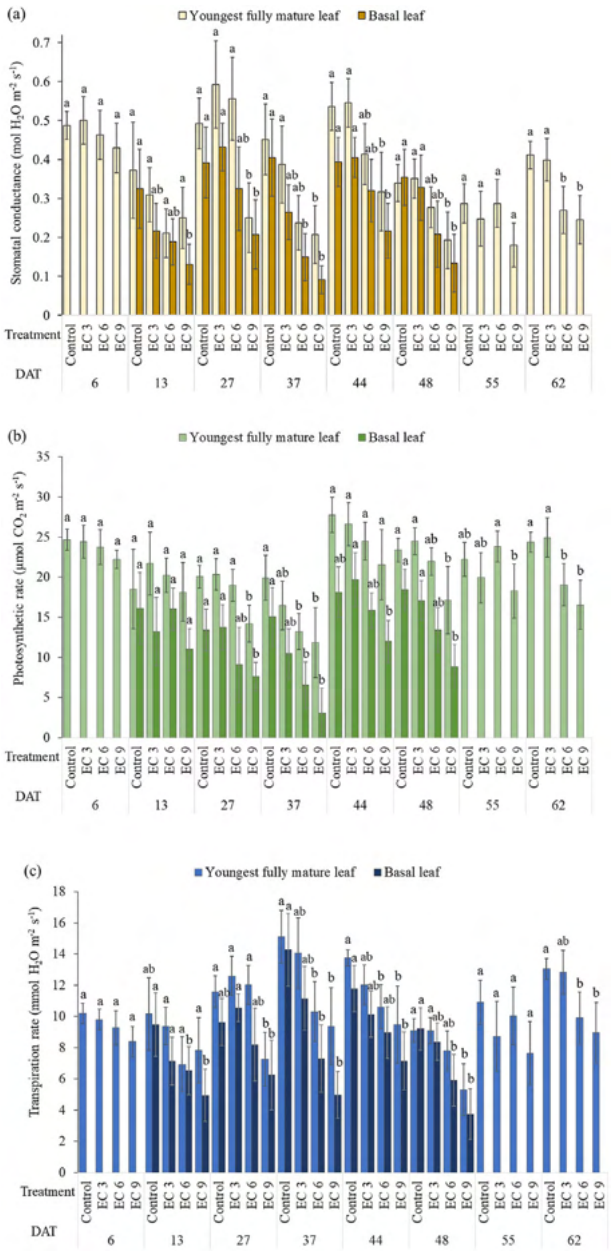

Fig. 2 – Stomatal conductance (a), photosynthetic rate (b), and transpiration rate (c) results in tomato plants under salt stress treatments (control, EC3, EC6, and EC9) ($n = 543$). Graphs are divided by measurement dates and present the youngest fully mature leaves and the basal leaves. Averages are shown with error bars of the confidence interval ($p \leq 0.05$). Letters represent significant differences between the youngest fully mature leaves and the basal leaves separately for the different treatments on the same DAT.

Photosystem II efficiency (PhiPS2) generally increased for the control, EC 3, and EC 6 throughout the experiment until 48 DAT. PhiPS2 for the EC 9 treatment did not show any significant change after 13 DAT. The average PhiPS2 difference between the youngest fully mature leaves and the basal leaves increased throughout the experiment.

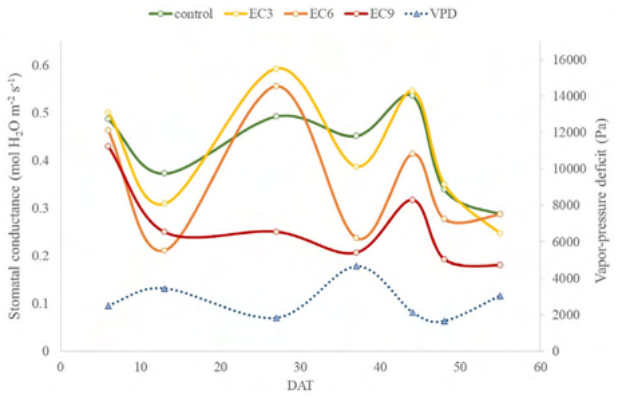

Fig. 3 – Changes in average stomatal conductance for the youngest fully mature leaf ($n = 90$) and leaf vapour pressure deficit on the day of sampling in the function of DAT for tomato plants under control, EC 3, EC 6, and EC 9 treatments.

3.3. *Internal content analysis*

Chloride concentration in both the youngest fully mature leaves and the basal leaves increased throughout the experiments (Fig. 4). In the first experiment (Fig. 4a), the older leaves continued accumulating Cl^- and did not reach saturation, while the youngest fully mature leaves maintained a similar trend but had lower chloride concentrations. Chloride differences became significant between treatments as the DAT progressed. In the second experiment (Fig. 4b), the plants showed similar Cl^- accumulation rates and differences between EC 3 and EC 9 in the upper and basal leaves as in the first experiment. Similarly to chloride, the sodium concentration in the leaves (Fig. 5) demonstrated significant differences between all treatments for the youngest fully mature leaves. Significant differences were also seen between the Na^+ concentrations of the control and EC 3 and between EC 3 and EC 6 and EC 9 for the older leaves.

The ratio of K^+ to Na^+ significantly decreased between all treatments for the youngest fully mature leaves (Fig. 6). The significance of the ratio was also demonstrated for the old leaves between the control and EC 3, EC 6, and between EC 3 and EC 6 and EC 9.

Sodium was found to be in an exponential positive correlation with chloride content in leaves. Treatments with a reduced concentration of NaCl (i.e., control and EC 3) demonstrated distinct accumulations of Cl^-, while the Na^+ accumulation was negligible. The exponential correlation yielded 0.72, 0.59, 0.76, and 0.41 coefficients of determination for the EC 9, EC 6, EC 3, and control treatments, respectively. The accumulation rate of Na^+ and Cl^- accelerated as higher salinity treatments were applied (Fig. 7).

3.4. *Spectral data analysis*

Average of the relative reflectance spectra of the youngest fully mature leaves and the basal leaves are presented for the first (Fig. 8 a-d) and second (Fig. 8 e-h) experiments. The presented spectral signatures are an average of all measurements

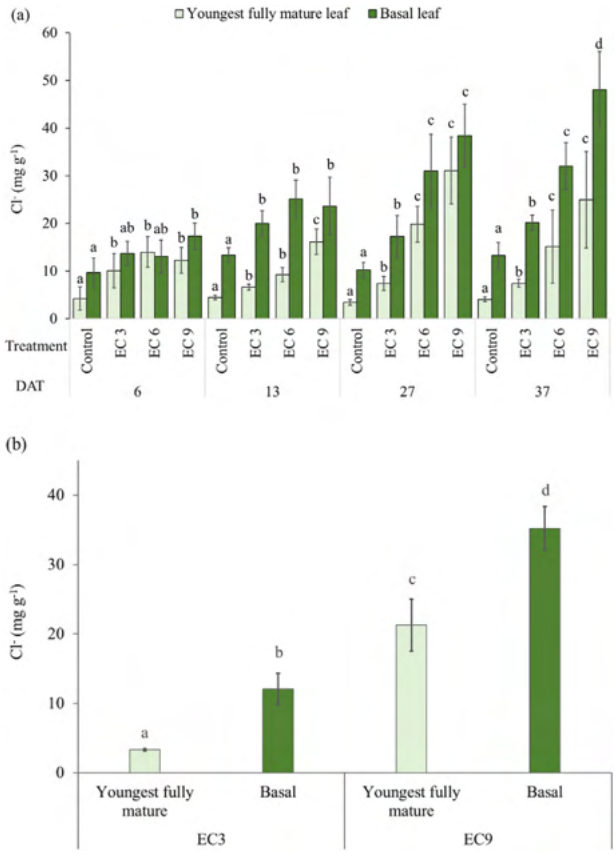

Fig. 4 – Cl^- concentration in tomato plants under salt stress treatments. The first experiment ($n = 154$) (a) shows control, EC3, EC6, and EC9 treatments by DAT, and the second experiment ($n = 24$) (b) depicts EC 3 and EC 9 treatments at 28 DAT for the youngest fully mature leaves and basal leaves. Averages are shown with error bars of the confidence interval ($p \leq 0.05$). Letters represent significant differences between the youngest fully mature leaves and the basal leaves separately for the different treatments on the same DAT.

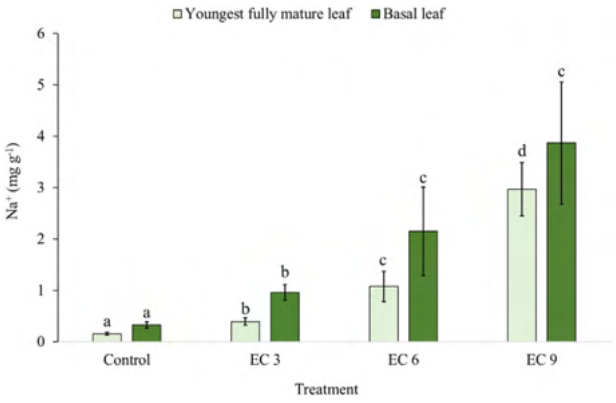

Fig. 5 – Na^+ concentration in tomato plants under salt stress treatments (control, EC3, EC6, and EC9) on 27 DAT for the youngest fully mature leaves and basal leaves' location ($n = 73$). Averages are shown with error bars of the confidence interval ($p \leq 0.05$). Letters represent significant differences between the youngest fully mature leaves and the basal leaves separately for the different treatments.

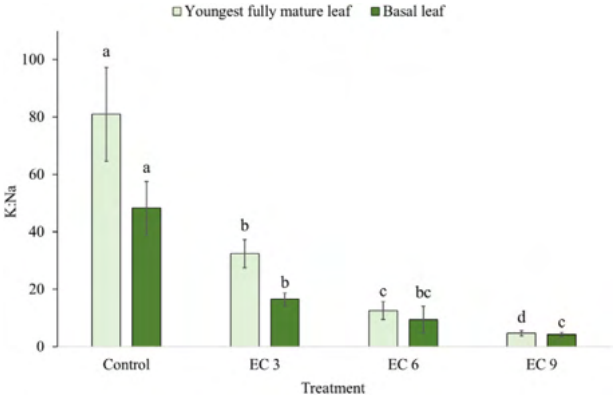

Fig. 6 – The K^+ to Na^+ ratio in tomato plants under salt stress treatments (control, EC3, EC6, and EC9) on 27 DAT for the youngest fully mature leaves and the basal leaves ($n = 73$). Averages are shown with error bars of the confidence interval ($p \leq 0.05$). Letters represent significant differences between the youngest fully mature leaves and the basal leaves separately for the different treatments.

taken throughout the experiment for the salt treatments. Reflectance curves of treatments for the youngest fully mature leaves are well separated (Fig. 8b, f) by an increase in the NIR reflectance as a function of the increasing salt concentrations.

in the irrigation water. In the visible spectrum, leaves under the control treatment demonstrated a higher spectral reflectance increase at 530–550 nm compared to the other treatments. The average relative reflectance from 600 to 700 nm was higher but not significant for the EC 6 and EC 9 than for the moderate salt treatments (control and EC 3). Basal leaves in the first experiment (Fig. 8d) under the control treatment showed slightly higher reflectance than all other treatments from 990 to 1120 nm, while this trend could not be observed in the second experiment.

To enhance the spectral signature differences and in order to find the highest variance in the spectra, several pre-processing methods were applied. The second derivative of the relative reflectance showed the greatest differences among the treatments. The 500–600 nm spectral range was selected to demonstrate these differences in Fig. 9. An increasing local amplitude fluctuation can be observed in the second derivative of the leaf reflectance as higher saline treatments were applied. Therefore, throughout the chemometric data analysis, the Savitzky–Golay (Savitzky & Golay, 1964) second derivative (window size: 7, polynomial order: 2) of the relative reflectance was applied for the full spectral range.

A combined PLS-R model was established, predicting Na^+ and Cl^- content simultaneously based on the hyperspectral signature in the range of 400–1800 nm. The Na^+ calibration model resulted within RMSEC of 0.48 mg g^{-1}, RMSECV of 0.69 mg g^{-1} along with R^2 Cal and CV 0.82 and 0.63, respectively, while the Cl^- calibration model resulted within RMSEC

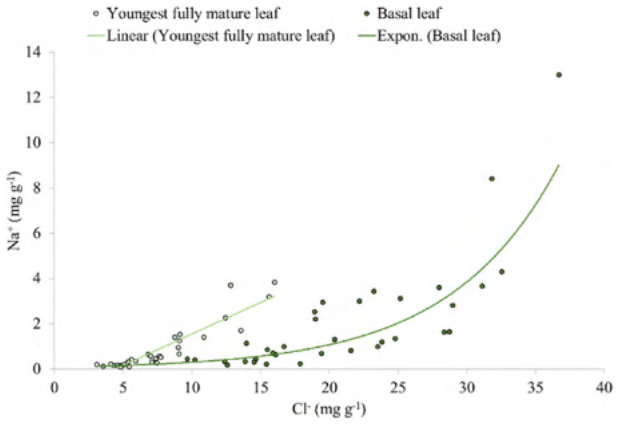

Fig. 7 – Trends of sodium content change with the increasing chloride concentration in the upper and basal leaves ($n = 73$) on 27 DAT. Liner line: $y = 0.2785x - 1.2418$, R^2 (determination coefficient) = 0.84 and exponential line: $y = 0.0844e^{0.1273x}$, $R^2 = 0.70$.

of 2.1 mg g^{-1}, RMSECV of 2.9 mg g^{-1} along with R^2 Cal and CV 0.75 and 0.52, respectively. The prediction model using four latent variables (LV) resulted within RMSEP of 0.47 mg g^{-1} and 2.8 mg g^{-1} for Na^+ and Cl^-, respectively along with R^2 (Pred) of 0.79 and 0.75 for Na^+ and Cl^-, respectively. These results are depicted in Fig. 10a and Fig. 10b for the youngest fully mature leaves on 27 DAT for Na^+ and Cl^-, respectively. Additionally, an efficient prediction model was established for K:Na ratio prediction within RMSEP 12.7, which is the 10% error of the measured K:Na ratio range (Fig. 10c). The K:Na regression model built with 4 LVs resulted within RMSEC of 9.4, RMSECV of 18.9 along with R^2 Cal and CV 0.89 and 0.58, respectively while R^2 Pred was 0.83. The variable importance in projection (VIP) was derived from the PLS-R analysis and was used for obtaining the significant wavebands related to the ion (Cl^-, Na^+) contents (Fig. 11 a, b) and the K:Na ratio (Fig. 11 c). The most sensitive wavelength ranges for Cl^- were 500–531, 682–752, 1310–1407, and 1763–1768 nm, while for Na^+, they were mainly the 500–531 and 682–752 nm wavebands. Additionally, the 986 and 1766 nm bands appeared in the ion content prediction models. In case of K:Na, the 500–533, 561–585, 682–752, and 986 nm wavebands significantly contributed to the regression models.

For the evaluation of leaf age and environmental conditions independent of internal component measurements, a PLS-R prediction model, combining the youngest fully mature leaves and basal leaves for Cl^- throughout three measurement campaigns, was established. It resulted in 6 LVs, RMSEC 5.1 mg g^{-1}, RMSECV 8.4 mg g^{-1}, RMSEP 6.9 mg g^{-1}, R^2 (Cal, CV) = 0.84, 0.58, and R^2 (Pred) = 0.69 (Fig. 12).

The robustness of the established regression model was studied by applying it to relative reflectance datasets that were collected in the second salt stress experiment. The performance of the PLS-R prediction model (Fig. 13), for Cl^- content detection, yielded 4 LVs, RMSEC 4.2 mg g^{-1}, RMSECV 6.1 mg g^{-1}, RMSEP 7.5 mg g^{-1}, R^2 (Cal, CV) = 0.84, 0.67, and R^2 (Pred) = 0.69.

The PLS-DA classification was applied to detect plant saline stress and to create a detection support classification model. The classification model performance is presented in Fig. 14. The PLS-DA model was able to correctly predict 71% of the

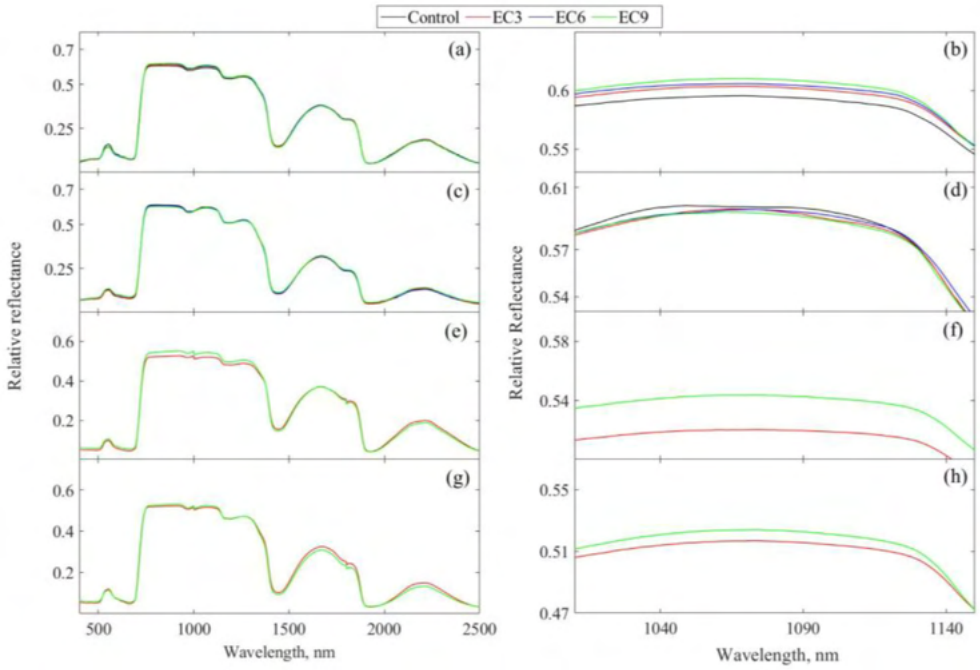

Fig. 8 – Averaged relative reflectance of all measurement days for the control, EC 3, EC 6, and EC 9 treatments. Spectral signature for 400–2500 nm for the youngest fully mature leaves (a: first experiment, e: second experiment) and basal (c: first experiment, g: second experiment) leaves along with a focus on areas with major differences between treatments (youngest fully mature leaves (b: first experiment, f: second experiment), basal leaves (d: first experiment, h: second experiment).

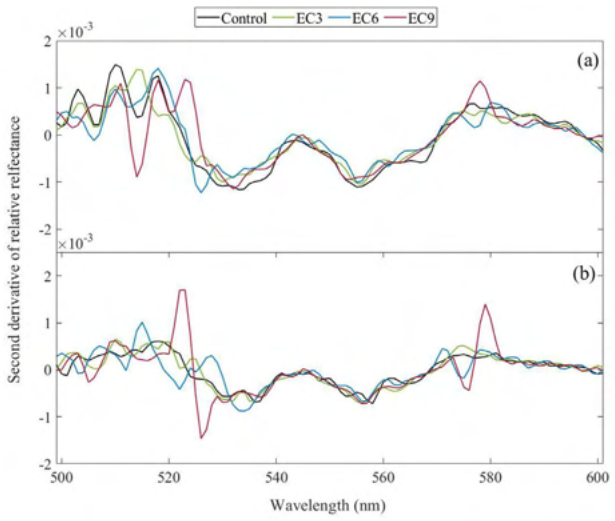

Fig. 9 – Plot of pre-processed (Savitzky–Golay second derivative with window size: 7 and polynomial order: 2) relative reflectance spectrum for the control, EC 3, EC 6, and EC 9 treatments in the range of 500–600 nm for the youngest fully mature leaves (a) and the basal leaves (b) on June 4, 2018.

non-stressed (sensitivity) and 94% of the stressed samples (specificity) using 7 LVs. The calibration and cross-validation results of the classification model were as follows: Sensitivity (Cal) = 1, Specificity (Cal) = 0.99, Sensitivity (CV) = 0.73, and Specificity (CV) = 0.86.

4. Discussion

The results presented in this work demonstrated how salt stress in grafted tomato plants can be monitored: (1) in a non-destructive manner by using hyperspectral measures; (2) disregarded according to leaf age and location; and (3) independently from environmental changes.

4.1. *Physiological performance and internal content*

The physiological performance of tomato leaves throughout the experiment showed a decreasing trend as a function of the salt stress introduced to the plants. The g_s demonstrated an oscillating rhythm that was affected by meteorological factors, such as VPD_{air}, temperature, and humidity. These results are in line with the findings of (Maroco et al., 1997; Hernandez et al., 2016) in *Eucalyptus globulus*. Under mild salt treatments (i.e., control and EC 3), a decreasing trend of g_s difference of the youngest fully mature leaves and basal leaves might have been due to the excessive Na^+ and Cl^- ion concentrations in the leaves of plants that were under salinity treatments, causing decreased water content and, thus, resulting in earlier stomatal closure (Munns, 2005). The photosynthetic rate (P_N) showed a similar decreasing trend to g_s except that on several measurement dates, EC 3-treated plants demonstrated P_N that was equal to or higher than the control treatment. These results suggest that low salt concentrations, with EC such as 3 dS m^{-1}, may not cause noticeable physiological differences (Cuartero & Fernández-Muñoz, 1998). The temporally increasing P_N ratio of the youngest fully mature leaves and basal leaves revealed that the salt accumulation in the bottom leaves affected their photosynthetic ability (Munns, 2002; Tavakkoli et al., 2011; Di Gioia et al., 2013). Although the transpiration rate (E) was very similar in its trends to g_s, on 37 DAT, E showed a high rate of activity while stomatal conductance decreased. This behaviour can be explained by the climatic conditions of that particular day, when the maximum temperature reached 41.2 °C, along with a very low relative humidity, dropping to ~16% (Fig. 1). Under these conditions, the evaporative environmental demand is very high, leading to a high transpiration rate, but the plant reduces the g_s by closing the stomata (Munns, 2005). Similar trends were found in rice (Singh & Sasahara, 1981), African

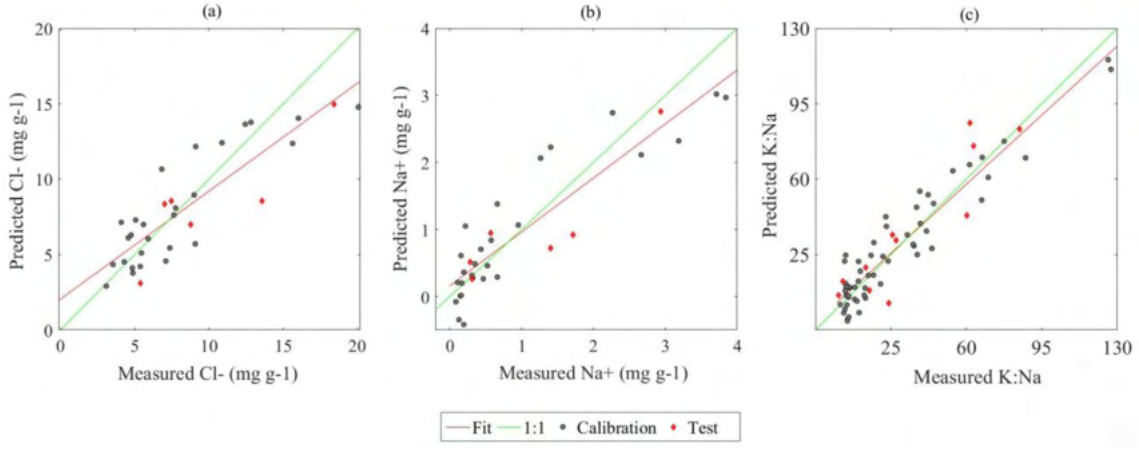

Fig. 10 – Scatter plots of the combined PLS-R regression model results of predicted Cl^- (a) and Na^+ (b) contents and for the K:Na ratio (c) versus the laboratory measurements. Cl^- and Na^+ shown for the youngest fully mature leaves ($n = 40$) on 27 DAT and for the K:Na ratio ($n = 73$) on 27 and 34 DAT. The Cl^- and Na^+ model is based on the pre-treated relative reflectance spectra in the spectral range of 400–1800 nm and for the K:Na ratio at 500–1100 nm.

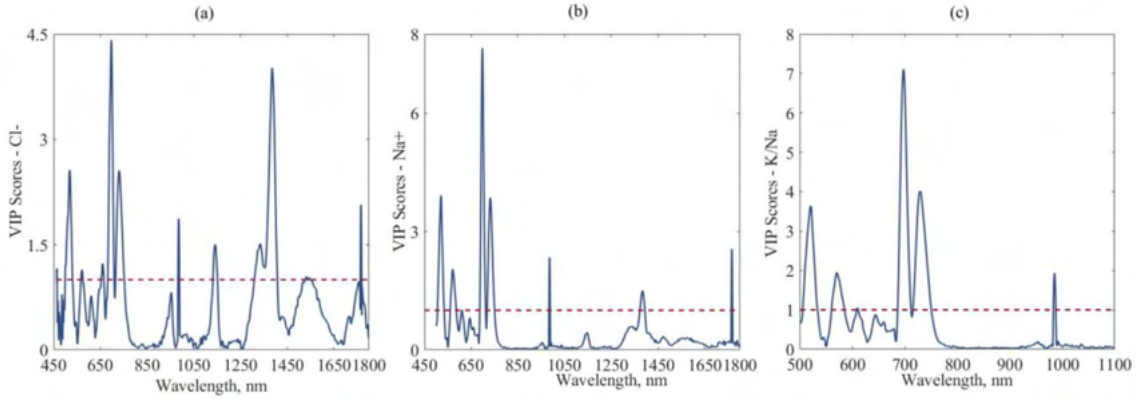

Fig. 11 – Variable importance in projection in the function of wavelengths for the PLS-R prediction models of Cl- (a), Na^+ (b), and K:Na (c).

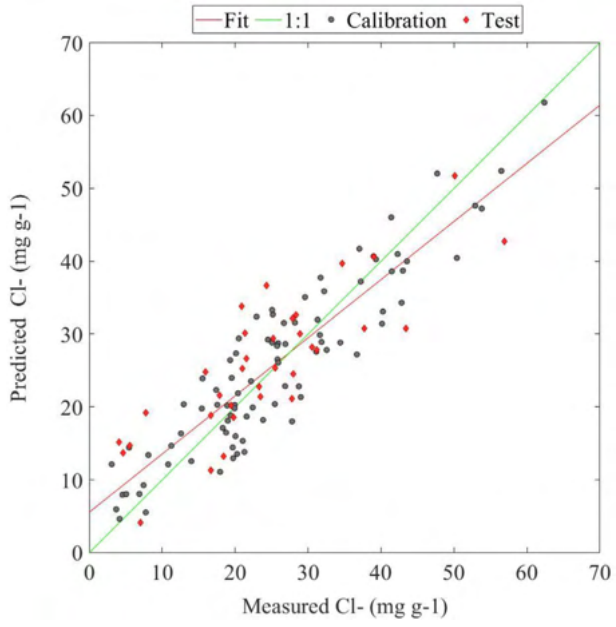

Fig. 12 – Scatter plot of PLS-R regression model results of predicted Cl^- content versus the laboratory measurements for both upper and lower leaves throughout three measurement campaigns ($n = 134$). The model is based on the pre-treated relative reflectance spectra in the spectral range of 400–1800 nm.

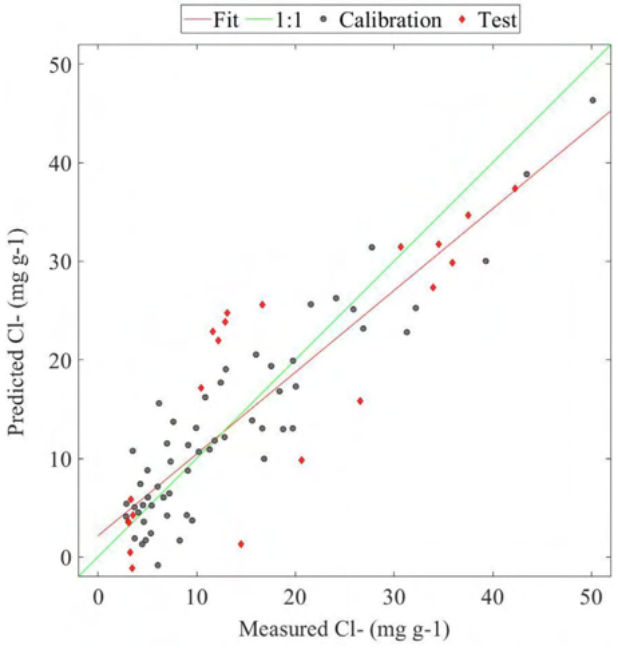

Fig. 13 – Application of the established PLS-R, Cl^- prediction model to the reflectance data of the second experiment for the youngest fully mature leaves ($n = 73$). The model is based on the pre-treated relative reflectance spectra in the spectral range of 400–1800 nm.

grasses (Maroco et al., 1997), and Armenian plums (Schulze et al., 1975). Though these environmental conditions are extreme, still, significant differences in the transpiration rate were obtained between treatments, indicating the effect of the salt accumulation on the plants' ability to physiologically function under stress. The general increase in PhiPS2, for all treatments until 48 DAT, except for the EC 9 treatment, which did not show any significant change after 13 DAT, suggests that the excessive amounts of NaCl caused almost immediate damage to the photosystem II complex, decreasing its photosynthetic activity (Mehta et al., 2010). The differences between the behaviours of the upper and lower leaves suggest that salt accumulation may significantly influence the functioning of photosystem II. A decrease in C_i was shown in the literature to be a typical physiological response of plants under salt stress (Downton et al., 1985) and in a linear relation with internal leaf Cl^- (Seemann & Critchley, 1985), which can explain the gradual decrease in C_i. The growing internal composition in aged leaves demonstrated that cellular compartmentalisation of salts predominantly occurred in the older leaves, reaching a chloride concentration of 50–70 mg g^{-1}. Photosystem II activity measurements demonstrated that the youngest fully mature leaves performed better than old leaves under all treatments, a

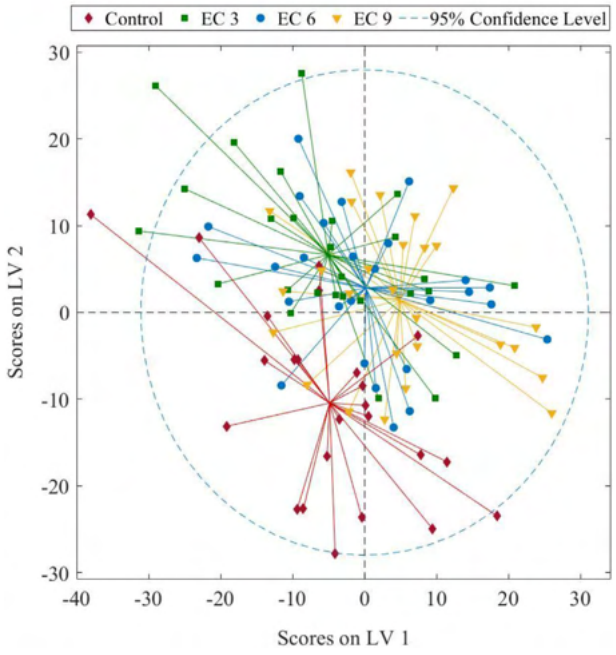

Fig. 14 – Scatter plot of PLS-DA classification model results of predicted class membership for both upper and lower leaves throughout four measurement campaigns ($n = 197$). The model is based on the pre-treated (D_2R) relative reflectance spectra in the spectral range of 400–1800 nm.

behaviour that may explain the plant's systematic storing of salts in bottom leaves as a defence mechanism to cope with salt stress (Niu et al., 1995). The decreasing ratio of K^+ to Na^+ between treatments in the young leaves, in comparison to Na^+ concentration, indicates that the high quantity of salt in the system not only affected the physiological performance of the plant but also reduced K^+ uptake (Cuartero et al., 1992; Pérez-Alfocea et al., 1996). The presented physiological and biochemical results suggest that the magnitude in which physiological variables perform have a great dependence on environmental variables and are not solely salt-treatment-related.

4.2. *Spectral signature*

Relative reflectance obtained from tomato leaves manifested changes as a function of increasing salt concentrations. The youngest fully mature leaves demonstrated spectral changes on different wavelengths compared to the basal leaves. Leaf reflectance tendencies in the NIR region, due to increases in soil salinity, are not uniform in the literature. Previous works in eggplant and barley showed a decrease (Peñuelas et al., 1997; Leone et al., 2007), while melon plants demonstrated an increase in NIR reflectance as a function of salinity (Hernández et al., 2014). Similarly, Zhang et al. (2011) detected a rise in NIR reflectance for salt-tolerant species growing in moderately saline soils. The results presented by Zhang et al. (2011) and Hernández et al. (2014) are consistent with the findings of this work. In general, higher NIR reflectance is associated with normal plant development (Jensen, 1983). The broad trend of NIR reflectance reduction appeared suitable for describing the salt stress effects on non-tolerant plant species but was not satisfactory for salt-tolerant plants growing in moderately saline soils (Läuchli & Lüttge, 2002; Zhang et al., 2011). As suggested in the literature, tomato, being salt-tolerant in comparison with other agricultural crops, has also been shown to act as salt-tolerant in a spectral manner.

4.3. *Machine learning*

PLS-R models related the spectral information to the internal composition of leaves under salinity treatments. As discussed above, it is important to monitor Na^+ and Cl^- due to their different trends concerning ion accumulation in leaves and the potassium and sodium ratio as it influences physiological performance and K^+ uptake. The hyperspectral measurement-based PLS-R model for predicting Na^+ and Cl^- content in upper leaves showed the ability of spectroscopy for salinity stress detection in a non-destructive manner. Along with Cl^- accumulation, the K:Na ratio was found to be a useful measure for salinity stress in plants (Tavakkoli et al., 2011). The established K:Na ratio prediction model enabled the non-destructive spectral monitoring of Na^+ toxicity and competition for the K^+ binding site. The important wavebands in the Cl^-, Na^+ and K:Na prediction models were in line with the findings of El-Hendawy et al. (2019) for wheat irrigated with saline water. Moreover, the 986-nm band was found to significantly contribute to these prediction models, suggesting the role played by starch content differences in the increasing ion contents. The change in starch content is related to photo-assimilated carbon storage, which, according to the literature, is influenced by plant abiotic stress (Thalmann & Santelia, 2017). Generally, in vegetation stress measurements, the youngest fully mature leaf is investigated. Defining "youngest fully mature leaf" is a subjective matter and depends on the proficiency of the sampler. The spectral signature is influenced by the structure of the leaf, which, among other factors, is age-related. This phenomenon leads to greater diversity in the spectral signatures. Taking into consideration that the chemometric models are applied to a great diversity of leaves, a prediction model should preferably be leaf-age-independent. Moreover, the plant physiological state that was discussed above is greatly dependent on environmental conditions, together with the consequences of salt stress. Due to the environmental condition diversity, the temporal stress trend analysis, based on physiological variables, was not feasible. Therefore, it is essential to examine the ability of spectral measurements, particularly regarding whether they are independent of daily environmental changes when analysing plant stress caused by ion accumulation in the leaves. The PLS-R model that predicted Cl^- content, including the reflectance of leaves of various ages from different measurement regimes under environmental and temporal influences, resulted within a RMSEP of 6.9 mg g^{-1}. The robustness of the established regression model and its applicability was evaluated by testing it on an independent dataset, resulting within a RMSEP of 7.5 mg g^{-1}. Although the prediction error was slightly higher than that of the previous models, it should be noted that the model was applied to a different tomato

cultivar. This suggests that in order to improve the prediction ability of the original model, it should be trained with additional tomato cultivars. The results demonstrate an ability to establish a robust prediction model for plant stress detection in diverse environmental conditions. These achievements advance the approach of Leone et al. (2007), for which plant spectral signature was related to soil salinity, as well as the work of Goldshleger et al. (2013), which linked plant Na^+ and Cl^- contents to saline soil spectral signatures.

PLS-R prediction models were established in order to quantify the amount of accumulated salt ions in the leaves, indicating the level of plant stress. For practical application, it is more important to determine whether a plant suffers from salt stress than the accumulated amount of salt in the leaves. The PLS-DA classification, based on hyperspectral measurements, showed great ability to efficiently distinguish the non-stressed from the saline-stressed tomato plants with high specificity and sensitivity.

5. Conclusion

Salt treatments were found to affect the physiological performance of plants, although environmental conditions had a greater influence on plant temporal physiological trends. Spectral data acquisition with machine learning showed high ability to predict salt accumulation in plants. Moreover, a hyperspectral, robust decision-supporting classification model was established for detecting plants under salt stress. The presented capabilities of predicting Cl^-, Na^+, and the K:Na ratio in a non-destructive manner, by utilizing spectroscopy, could serve as the basis for developing a low-cost, fast, and efficient stress detection method, independent of environmental conditions.

Further research is required to improve the prediction model accuracy by extending the dataset with additional cultivars and in more diverse environmental conditions. Furthermore, regarding the practical application, a reduced variable model for multispectral imaging could be developed in order to enable salt stress monitoring in a commercial manner.

Author contributions

Timea Ignat: conceptualisation, methodology, software, data curation, investigation, formal analysis, supervision, writing: original draft preparation, writing: reviewing and editing. **Yoav Shavit**: conceptualisation, methodology, software, data curation, investigation, formal analysis, writing: original draft preparation. **Shimon Rachmilevitch:** conceptualisation, supervision, reviewing. **Arnon Karnieli**: conceptualisation, supervision, reviewing.

Declaration of competing interest

The authors declare that they have no known competing financial interests or personal relationships that could have appeared to influence the work reported in this paper.

Acknowledgements

This research was supported by the Ministry of Agriculture and Rural Development, Israel (Eugene Kandel Knowledge Centres) as part of the Root of the Matter project: The Root Zone Knowledge Centre for Leveraging Modern Agriculture (391/15/16-34-0005).

REFERENCES

Ahmad, P., Jaleel, C. A., Salem, M. A., Nabi, G., & Sharma, S. (2010). Roles of enzymatic and nonenzymatic antioxidants in plants during abiotic stress. *Critical Reviews in Biotechnology, 30*(3), 161–175. https://doi.org/10.3109/07388550903524243

Aidoo, M. K., Sherman, T., Ephrath, J. E., Fait, A., Rachmilevitch, S., & Lazarovitch, N. (2018). Grafting as a method to increase the tolerance response of bell pepper to extreme temperatures. *Vadose Zone Journal, 17*(1), 170006. https://doi.org/10.2136/vzj2017.01.0006

Brunner, V., Siegl, M., Geier, D., & Becker, T. (2021). Challenges in the development of soft sensors for bioprocesses: A critical review. *Frontiers in Bioengineering and Biotechnology, 9*, 1–21. https://doi.org/10.3389/fbioe.2021.722202. August.

Campbell, C. R., & Plank, C. O. (1998). Preparation of plant tissue for laboratory analysis. In *Handbook of Methods for Plant Analysis* (Vol. 38, Issue 6, pp. 37–50). https://doi.org/10.2135/cropsci1998.0011183X003800060050x.

Carter, G. A., & Knapp, A. K. (2001). Leaf optical properties in higher plants: Linking spectral characteristics to stress and chlorophyll concentration. *American Journal of Botany, 88*(4), 677–684. https://doi.org/10.2307/2657068

Cochavi, A., Rapaport, T., Gendler, T., Karnieli, A., Eizenberg, H., Rachmilevitch, S., & Ephrath, J. E. (2017). Recognition of orobanche cumana below-ground parasitism through physiological and hyper spectral measurements in sunflower (Helianthus annuus L.). *Frontiers of Plant Science, 8*, 1–12. https://doi.org/10.3389/fpls.2017.00909. June.

Cuartero, J., & Fernández-Muñoz, R. (1998). Tomato and salinity. *Scientia Horticulturae, 78*(1–4), 83–125. https://doi.org/10.1016/S0304-4238(98)00191-5

Cuartero, J., Yeo, A. R., & Flowers, T. J. (1992). Selection of donors for salt-tolerance in tomato using physiological traits. *New Phytologist, 121*(1), 63–69. https://doi.org/10.1111/j.1469-8137.1992.tb01093.x

Dalton, F. N., Maggio, A., & Piccinni, G. (2001). Assessing the effect of solar radiation on plant salt tolerance as defined by the static and dynamic indices. *Plant and Soil, 229*(2), 189–195. https://doi.org/10.1023/A:1004891301238

Das, B., Manohara, K. K., Mahajan, G. R., & Sahoo, R. N. (2020). Spectroscopy based novel spectral indices, PCA- and PLSR-coupled machine learning models for salinity stress phenotyping of rice. *Spectrochimica Acta Part A: Molecular and Biomolecular Spectroscopy, 229*, 117983. https://doi.org/10.1016/j.saa.2019.117983

Di Gioia, F., Signore, A., Serio, F., & Santamaria, P. (2013). Grafting improves tomato salinity tolerance through sodium partitioning within the shoot. *HortScience, 48*(7), 855–862. https://doi.org/10.21273/hortsci.48.7.855

Downton, W. J. S., Grant, W. J. R., & Robinson, S. P. (1985). Photosynthetic and stomatal responses of spinach leaves to salt stress. *Plant Physiology, 78*(1), 85–88. https://doi.org/10.1104/pp.78.1.85

El-Hendawy, S. E., Al-Suhaibani, N. A., Hassan, W. M., Dewir, Y. H., Elsayed, S., Al-Ashkar, I., Abdella, K. A., & Schmidhalter, U.

(2019). Evaluation of wavelengths and spectral reflectance indices for high-throughput assessment of growth, water relations and ion contents of wheat irrigated with saline water. *Agricultural Water Management, 212*, 358–377. https://doi.org/10.1016/j.agwat.2018.09.009. April 2018.

Estañ, M. T., Martinez-Rodriguez, M. M., Perez-Alfocea, F., Flowers, T. J., & Bolarin, M. C. (2005). Grafting raises the salt tolerance of tomato through limiting the transport of sodium and chloride to the shoot. *Journal of Experimental Botany, 56*(412), 703–712. https://doi.org/10.1093/jxb/eri027

FAOSTAT. (2018). *Faostat*.

Gausman, H. W. (1984). Evaluation of factors causing reflectance differences between Sun and Shade Leaves. *Remote Sensing of Environment, 15*(2), 177–181. https://doi.org/10.1016/0034-4257(84)90045-2

Goldshleger, N., Chudnovsky, A., & Ben-Binyamin, R. (2013). Predicting salinity in tomato using soil reflectance spectra. *International Journal of Remote Sensing, 34*(17), 6079–6093. https://doi.org/10.1080/01431161.2013.793859

Grunberg, K., Fernández-Muñoz, R., & Cuartero, J. (1995). Growth, flowering, and quality and quantity of pollen of tomato plants grown under saline conditions. *Acta Horticulturae, 412*, 484–489. https://doi.org/10.17660/ActaHortic.1995.412.58

Hasegawa, P. M., Bressan, R. A., Zhu, J. K., & Bohnert, H. J. (2000). Plant cellular and molecular responses to high salinity. *Annual Review of Plant Biology, 51*, 463–499. https://doi.org/10.1146/annurev.arplant.51.1.463

Hernández, E. I., Melendez-pastor, I., Navarro-pedreño, J., & Gómez, I. (2014). Hernández et al. Spectral detection of melon nutrition. *Scientia Agricola*, 324–330. https://doi.org/10.1590/0103-9016-2013-0338. August.

Hernandez, M. J., Montes, F., Ruiz, F., Lopez, G., & Pita, P. (2016). The effect of vapour pressure deficit on stomatal conductance, sap pH and leaf-specific hydraulic conductance in Eucalyptus globulus clones grown under two watering regimes. *Annals of Botany, 117*(6), 1063–1071. https://doi.org/10.1093/aob/mcw031

Herrmann, I., Bdolach, E., Montekyo, Y., Rachmilevitch, S., Townsend, P. A., & Karnieli, A. (2020). Assessment of maize yield and phenology by drone-mounted superspectral camera. *Precision Agriculture, 21*(1), 51–76. https://doi.org/10.1007/s11119-019-09659-5

Hsiao, T. C. (1973). Plant responses to water stress. *Annual Review of Plant Biology, 24*, 519–570.

Jensen, J. R. (1983). Review article: Biophysical remote sensing. *Annals of the Association of American Geographers, 73*(1), 111–132. https://doi.org/10.2307/2569349

Johnson, R. W., Dixon, M. A., & Lee, D. R. (1992). Water relations of the tomato during fruit growth. *Plant, Cell and Environment, 15*(8), 947–953. https://doi.org/10.1111/j.1365-3040.1992.tb01027.x

Kaur, G., Kumar, S., Nayyar, H., & Upadhyaya, H. D. (2008). Cold stress injury during the pod-filling phase in chickpea (Cicer arietinum L.): Effects on quantitative and qualitative components of seeds. *Journal of Agronomy and Crop Science, 194*(6), 457–464. https://doi.org/10.1111/j.1439-037X.2008.00336.x

Kubota, C., McClure, M. A., Kokalis-Burelle, N., Bausher, M. G., & Rosskopf, E. N. (2008). Vegetable grafting: History, use, and current technology status in North America. *HortScience, 43*(6), 1664–1669. https://doi.org/10.21273/hortsci.43.6.1664

Läuchli, A., & Lüttge, U. (2002). Salinity: Environment – plants – molecules. In A. Läuchli, & U. Lüttge (Eds.), *Climate change 2013 - the physical science basis*. KLUWER ACADEMIC PUBLISHERS.

Lee, J. M., Kubota, C., Tsao, S. J., Bie, Z., Echevarria, P. H., Morra, L., & Oda, M. (2010). Current status of vegetable grafting: Diffusion, grafting techniques, automation. *Scientia Horticulturae, 127*(2), 93–105. https://doi.org/10.1016/j.scienta.2010.08.003

Lee, J.-M., & Oda, M. (2003). Grafting of herbaceous vegetable and ornamental crops. In *Horticultural reviews* (Vol. 28, pp. 61–124). John Wiley & Sons. https://doi.org/10.1002/9780470650851.ch2.

Leone, A. P., Menenti, M., Buondonno, A., Letizia, A., Maffei, C., & Sorrentino, G. (2007). A field experiment on spectrometry of crop response to soil salinity. *Agricultural Water Management, 89*(1–2), 39–48. https://doi.org/10.1016/j.agwat.2006.12.004

Maggio, A., Miyazaki, S., Veronese, P., Fujita, T., Ibeas, J. I., Damsz, B., Narasimhan, M. L., Hasegawa, P. M., Joly, R. J., & Bressan, R. A. (2002). Does proline accumulation play an active role in stress-induced growth reduction? *The Plant Journal, 31*(6), 699–712. https://doi.org/10.1046/j.1365-313X.2002.01389.x

Mantri, N., Patade, V., Penna, S., Ford, R., & Pang, E. (2012). Abiotic stress responses in plants: Present and future. In *Abiotic stress responses in plants* (pp. 1–19). New York: Springer. https://doi.org/10.1007/978-1-4614-0634-1_1.

Maroco, J. P., Pereira, J. S., & Chaves, M. M. (1997). Stomatal responses to leaf-to-air vapour pressure deficit in Sahelian species. *Australian Journal of Plant Physiology, 24*(3), 381–387. https://doi.org/10.1071/PP96062

Mehta, P., Jajoo, A., Mathur, S., & Bharti, S. (2010). Chlorophyll a fluorescence study revealing effects of high salt stress on Photosystem II in wheat leaves. *Plant Physiology and Biochemistry, 48*(1), 16–20. https://doi.org/10.1016/j.plaphy.2009.10.006

Morgan, J. M. (1984). *Plants. 30* pp. 299–319).

Munns, R. (2002). Comparative physiology of salt and water stress. *Plant, Cell and Environment, 25*(2), 239–250. https://doi.org/10.1046/j.0016-8025.2001.00808.x

Munns, R. (2005). Genes and salt tolerance: Bringing them together. *New Phytologist, 167*(3), 645–663. https://doi.org/10.1111/j.1469-8137.2005.01487.x

Niu, X., Bressan, R. A., Hasegawa, P. M., & Pardo, J. M. (1995). Ion homeostasis in NaCI stress environments. *Plant Physiology, 109*(3), 735–742. https://doi.org/10.1104/pp.109.3.735

Papadopoulos, I., & Rendig, V. V. (1983). Tomato plant response to soil salinity 1. *Agronomy Journal, 75*(4), 696–700. https://doi.org/10.2134/agronj1983.00021962007500040028x

Peñuelas, J., Isla, R., Filella, I., & Araus, J. L. (1997). Visible and near-infrared reflectance assessment of salinity effects on barley. *Crop Science, 37*(1), 198–202. https://doi.org/10.2135/cropsci1997.0011183X003700010033x

Pérez-Alfocea, F., Balibrea, M. E., Santa Cruz, A., & Estañ, M. T. (1996). Agronomical and physiological characterization of salinity tolerance in a commercial tomato hybrid. *Plant and Soil, 180*(2), 251–257. https://doi.org/10.1007/bf00015308

Pitman, M. G., & Läuchli, A. (2006). Global impact of salinity and agricultural ecosystems. *Salinity: Environment - Plants - Molecules*, 3–20. https://doi.org/10.1007/0-306-48155-3_1

Qadir, M., Quillérou, E., Nangia, V., Murtaza, G., Singh, M., Thomas, R. J., Drechsel, P., & Noble, A. D. (2014). Economics of salt-induced land degradation and restoration. *Natural Resources Forum, 38*(4), 282–295. https://doi.org/10.1111/1477-8947.12054

Rapaport, T., Hochberg, U., Shoshany, M., Karnieli, A., & Rachmilevitch, S. (2015). Combining leaf physiology, hyperspectral imaging and partial least squares-regression (PLS-R) for grapevine water status assessment. *ISPRS Journal of Photogrammetry and Remote Sensing, 109*, 88–97. https://doi.org/10.1016/j.isprsjprs.2015.09.003

Rodríguez-Pérez, J. R., Riaño, D., Carlisle, E., Ustin, S., & Smart, D. R. (2007). Evaluation of hyperspectral reflectance indexes to detect grapevine water status in vineyards. *American Journal of Enology and Viticulture, 58*(3), 302–317.

Romero-Aranda, R., Soria, T., & Cuartero, J. (2002). Greenhouse mist improves yield of tomato plants grown under saline

conditions. *Journal of the American Society for Horticultural Science, 127*(4), 644–648. https://doi.org/10.21273/jashs.127.4.644

Savitzky, A., & Golay, M. J. E. (1964). Smoothing and differentiation of data by simplified least squares procedures. *Analytical Chemistry, 36*(8), 1627–1639. https://doi.org/10.1021/ac60214a047

Savvas, D., Savva, A., Ntatsi, G., Ropokis, A., Karapanos, I., Krumbein, A., & Olympios, C. (2011). Effects of three commercial rootstocks on mineral nutrition, fruit yield, and quality of salinized tomato. *Journal of Plant Nutrition and Soil Science, 174*(1), 154–162. https://doi.org/10.1002/jpln.201000099

Schulze, E. D., Lange, O. L., Evenari, M., Kappen, L., & Buschbom, U. (1975). The role of air humidity and temperature in controlling stomatal resistance of Prunus armeniaca L. under desert conditions - III. The effect on water use efficiency. *Oecologia, 19*(4), 303–314. https://doi.org/10.1007/BF00348106

Schwarz, D., Rouphael, Y., Colla, G., & Venema, J. H. (2010). Grafting as a tool to improve tolerance of vegetables to abiotic stresses: Thermal stress, water stress and organic pollutants. *Scientia Horticulturae, 127*(2), 162–171. https://doi.org/10.1016/j.scienta.2010.09.016

Seemann, J. R., & Critchley, C. (1985). Effects of salt stress on the growth, ion content, stomatal behaviour and photosynthetic capacity of a salt-sensitive species, Phaseolus vulgaris L. *Planta, 164*(2), 151–162. https://doi.org/10.1007/BF00396077

Serrano, L., González-Flor, C., & Gorchs, G. (2010). Assessing vineyard water status using the reflectance based Water Index. *Agriculture, Ecosystems & Environment, 139*(4), 490–499. https://doi.org/10.1016/j.agee.2010.09.007

Singh, M. K., & Sasahara, T. (1981). Photosynthesis and transpiration in rice as influenced by soil moisture and air humidity. *Annals of Botany, 48*(4), 513–518. https://doi.org/10.1093/oxfordjournals.aob.a086155

Steidle Neto, A. J., Toledo, J. V., Zolnier, S., de Lopes, D. C., Pires, C. V., & Silva, T. G. F.d. (2017). Prediction of mineral contents in sugarcane cultivated under saline conditions based on stalk scanning by Vis/NIR spectral reflectance. *Biosystems Engineering, 156*, 17–26. https://doi.org/10.1016/j.biosystemseng.2017.01.003

Tavakkoli, E., Fatehi, F., Coventry, S., Rengasamy, P., & McDonald, G. K. (2011). Additive effects of Na+ and Cl- ions on barley growth under salinity stress. *Journal of Experimental Botany, 62*(6), 2189–2203. https://doi.org/10.1093/jxb/erq422

Thakur, P., Kumar, S., Malik, J. A., Berger, J. D., & Nayyar, H. (2010). Cold stress effects on reproductive development in grain crops: An overview. *Environmental and Experimental Botany, 67*(3), 429–443. https://doi.org/10.1016/j.envexpbot.2009.09.004

Thalmann, M., & Santelia, D. (2017). Starch as a determinant of plant fitness under abiotic stress. *New Phytologist, 214*(3), 943–951. https://doi.org/10.1111/nph.14491

Vorasoot, N., Songsri, P., Akkasaeng, C., Jogloy, S., & Patanothai, A. (2003). Effect of water stress on yield and agronomic characters of peanut (Arachis hypogaea L.). *Songklanakarin Journal of Science and Technology, 25*(3), 283–288.

Yancey, P. H. (2004). Compatible and counteracting solutes: Protecting cells from the dead Sea to the deep sea. *Science Progress, 87*(Pt 1), 1–24. https://doi.org/10.3184/003685004783238599

Zhang, T. T., Zeng, S. L., Gao, Y., Ouyang, Z. T., Li, B., Fang, C. M., & Zhao, B. (2011). Using hyperspectral vegetation indices as a proxy to monitor soil salinity. *Ecological Indicators, 11*(6), 1552–1562. https://doi.org/10.1016/j.ecolind.2011.03.025

Zhu, J. K. (2001). Plant salt tolerance. *Trends in Plant Science, 6*(2), 66–71. https://doi.org/10.1016/S1360-1385(00)01838-0

Zhu, J. K. (2002). Salt and drought stress signal transduction in plants. *Annual Review of Plant Biology, 53*, 247–273. https://doi.org/10.1146/annurev.arplant.53.091401.143329